255-Gbps PAM-8 O-band Transmission through 10-km SMF under 14-GHz Bandwidth Limitation Using MLSE Based on Nonlinear Channel Estimation with Cutdown Volterra Kernels.

Hiroki Taniguchi(1), Shuto Yamamoto(1), Masanori Nakamura(1), Yoshiaki Kisaka(1)

(1) NTT Network Innovation Laboratories, NTT Corporation, hiroki.taniguchi.ys@hco.ntt.co.jp

Abstract *We demonstrate 255-Gbps/λ PAM-8 transmission over 10-km with a BER below the 7% HD-FEC threshold under a 14-GHz bandwidth limitation and −6.3-ps/nm chromatic dispersion by applying MLSE based on nonlinear channel estimation with reduced computational complexity.*

Introduction

With the increasing use of cloud services in recent years, network traffic within and between data centres (DCs) is expected to increase at a rate of about 1.3 times per year[1]. At present, Ethernet is mainly used as the connection method within and between DCs. Currently 400GbE is standardized in IEEE802.3 and 800GbE/1.6TbE are planned for the 2020s[2]. The capacity of Ethernet has become high due to an increase in the modulation speed, symbol level and number of wavelength channels in intensity modulation schemes and direct detection (IM-DD) systems, realizing economical short-reach transmission. For 400GbE, 50-Gbps or 100-Gbps PAM-4 (4-level pulse-amplitude-modulation) and wavelength division multiplexing (WDM) are employed in the O-band. For 800GbE/1.6TbE, 200-Gbps PAM-4 (100 Gbaud) or PAM-8 (66.7 Gbaud) is required. This increase in modulation speed requires broader bandwidth digital-to-analog converters (DACs) and analog-to-digital converters (ADCs). Therefore, for economical next generation Ethernet, it is important to reduce the cost of high-speed DACs/ADCs and to use narrowband and low-cost devices. Recently, research on 200-Gbps transmission in PAM-8, which can be achieved at lower baud rates than PAM-4, has been reported[3]. In addition, bandwidth limitations due to the increased number of transmission systems using narrowband, low-cost devices and inter-signal interference (ISI) due to chromatic-dispersion (CD) caused by the increase in the number of wavelength channels cause the waveform of the received signal to be distorted. Therefore, there are several studies to address these problems of IM-DD systems such as Kramers-Kronig receiver and Tomlinson-Harashima precoding[4-5]. A channel equalization technique using maximum likelihood sequence estimation (MLSE), which is a powerful equalization method for obtaining correct transmission data from a received signal waveform that is linearly distorted by ISI, has been also investigated for short-reach optical transmission[6]. However, conventional MLSE has a problem: the channel-estimation error increases in transmission systems that include nonlinear responses, such as drivers and modulators. To solve these problems, we previously proposed and implemented a nonlinear MLSE (NL-MLSE) with a Volterra filter and demonstrated 200-G/λ class PAM-4 and PAM-8 transmissions[7-8]. However, the NL-MLSE has a problem in that the filter increases the computational complexity.

In this paper, we propose a simplified NL-MLSE to reduce the computational complexity of nonlinear ISI estimation. We also demonstrate 255-Gbps, PAM-8, and 10-km transmission using the NL-MLSE with a simplified Volterra filter.

NL-MLSE with cutdown Volterra kernels reference to kernel weights

Figure 1 shows a block diagram of the proposed method, the NL-MLSE with cutdown Volterra kernels with reference to kernel weights. The proposed method consists of MLSE and a feed-forward equalizer (FFE) installed at the stage preceding the MLSE. The FFE has not installed in our previous proposed method. The sampling phase of the output sequence of the FFE is equal to that of the transmitted sequence. In receiver-side DSP without a phase recovery function, as used in offline experiments, the sampling phase of the received signal sampled by ADC is

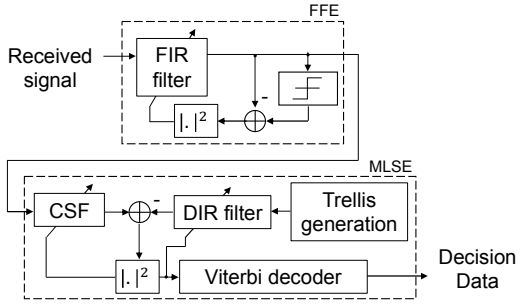

Fig. 1: Block diagram of NL-MLSE with cutdown Volterra kernels reference to kernel weights.

indefinite. The FFE has the role of fixing the sampling phase of the received signal.

In the NL-MLSE, a Volterra filter is applied to the desired impulse response (DIR) filter to estimate the nonlinear channel response. The output of an *m*-memory, third-order Volterra filter is expressed as

$$f(x_1,\cdots,x_m) = \sum_{a=1}^{m} k_a x_a + \sum_{a=1}^{m}\sum_{b=1}^{m} k_{ab} x_a x_b + \sum_{a=1}^{m}\sum_{b=1}^{m}\sum_{c=1}^{m} k_{abc} x_a x_b x_c \quad (1),$$

where $(x_1,\cdots,x_m)$ is a signal sequence such as the input of the DIR filter, and ($k_{1\sim m}$, $k_{11\sim mm}$, $k_{111\sim mmm}$) are kernels of the Volterra filter. In this case, the NL-MLSE has $\sum_{i=1}^{3} {}_{m+i-1}\mathrm{C}_i$ kernels and takes into account duplication. The amount of nonlinear calculation increases compared with the conventional MLSE, in which a linear filter is utilized as a DIR filter. Thus, this amount can be reduced while suppressing performance degradation by removing kernels in the order from the kernel with the smallest effect on the output of the Volterra filter, that is, the kernel with the smallest value.

To realize this method, it is necessary to fix the size relation of the kernels that changes depending on the sampling phase of the received signal sequence. The sampling phase of the channel shortening filter (CSF) input series is fixed by the FFE. Hence, the phase of the DIR filter, which is updated on the basis of a cost function with the CSF output, is also fixed. All kernels of the Volterra filter after the kernel update have a constant size relationship. In addition, the high-frequency signals that are suppressed in a transmission system are amplified with white noise by a finite impulse response (FIR) filter in the FFE. Therefore, the CSF suppresses the high-frequency components of the input sequence from the FFE.

Experiments and results

We experimentally evaluate the performance of the proposed simplified NL-MLSE in high-baud-rate PAM-8 transmission. Figure 2 shows the experimental setup. A transmission data sequence of 255-Gbps PAM-8 signals is generated by off-line DSP and a 32-GHz, 96-Gsample/s arbitrary waveform generator (AWG). In this experiment, a 15th-order pseudo-random binary sequence is utilized. The generated electrical signals are modulated to optical signals by a 30-GHz Mach-Zehnder modulator (MZM). The optical signals are transmitted over 10-km SMF without any optical amplifiers and received with a 50-GHz PIN photodiode (PD) after the received power is adjusted by a variable optical attenuator (VOA). The amount of chromatic dispersion is −6.3 ps/nm in the case of 10-km transmission at 1300.05 nm. The received signals are then converted into a digital signal sequence by a 65-GHz, 160-Gsample/s digital storage oscilloscope (DSO) and demodulated by the FFE and the MLSE with an FFE block. All of the FIR filter in the FFE have 45 T/2-spaced taps. The CSF and the DIR filter have 5 T-spaced taps. The FIR filters, CSF, and DIR filter are updated by the recursive least squares algorithm. To ensure the correct adaptation of the filters, the taps in the filters are trained beforehand by the first 1000 symbols. Figure 3 shows the frequency response of the transmission system. As shown in this figure, the 3-dB frequency bandwidth is 14 GHz.

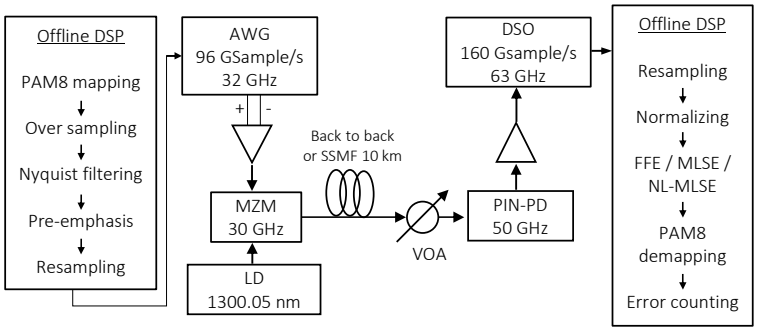

Fig. 2: Experimental setup.

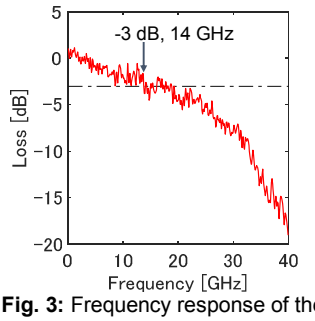

Fig. 3: Frequency response of the transmission system.

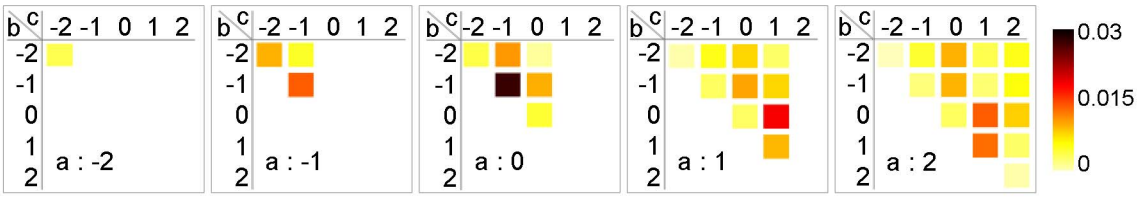

Fig. 4: Kernel weights (k_{abc}) of third-order in Volterra series after DIR filter convergence.

Figure 4 shows the 5-memory third-order kernel weights of the Volterra series after convergence of the DIR filter. In this case, there are ${}_7C_3 = 35$ third-order kernels. In Figure 4, k_{abc} represents the third-order kernels in the aforementioned equation (1), and the lightly coloredkernels with smaller values are removed from the k_{abc} when reducing the operation volume. For example, if 5-memory third-order Volterra kernels are reduced 20 kernels out of 35 (57%), multiplications and summations are omitted 60 out of 105 and 20 out of 34 per symbol, respectively.

Figure 5 shows the relationships between the received optical power and the BER in 10-km transmission for the FFE (FFE: triangle) and MLSEs with a FFE block that can estimate linear ISI (MLSE 1st: square), second-order nonlinear distortion (MLSE 2nd: diamond) and third-order nonlinear distortion (MLSE 3rd: circle). The dotted lines in this figure show the performances of the MLSEs in estimating third-order nonlinear distortion with the number of third-order Volterra kernels reduced from 57% to 86%. At the 7% HD-FEC threshold with a BER of 3.8E-3, compared with demodulation by the FFE, demodulation by MLSE 1st and MLSE 2nd improved the sensitivity by 0.8 dB, and demodulation by MLSE 3rd improved the sensitivity by 1.6 dB. When the number of third-order kernels is reduced by 57%, there is no penalty compared with the case without reduction, and a penalty starts to appear when the number of kernels is reduced by 71%, but even when the number of kernels is reduced by 86%, the penalty is limited to 0.4 dB.

Figure 6 shows the relationship between the rate of removing the number of third-order kernels and the transmission performance at a received power of 2 dBm, and it can be seen that performance degradation did not degrade even when up to 57% of the number of third-order kernels are removed in both back-to-back and 10 km transmissions. This shows that the proposed method reduces the amount of operation while minimizing the performance degradation of NL-MLSE.

Conclusions

We proposed a simplified NL-MLSE with reference to kernel weights. It has a BER below the 7% HD-FEC threshold for 255-Gb/s PAM8 signal, 10-km O-band transmission under a 14-GHz bandwidth limitation while maintaining performance equivalent to that of NL-MLSE with all third-order kernels. The research results we obtained lead us to conclude that a decoder using the simplified NL-MLSE effectively suppresses the increased nonlinear computational complexity in a high-baud-rate transmission system with higher-order PAM using narrow-band devices.

References

1. Cisco, “Cisco Global Cloud Index: Forecast and Methodology, 2016–2021”, 2018.
2. Ethernet Alliance, “The 2019 roadmap”, http://ethernetalliance.org, 2019.
3. F. Li *et al.*, “200 Gbit/s (68.25 Gbaud) PAM8 signal transmission and reception for intra-data center interconnect”, *Proc. OFC*, pp. W4I.3, 2019.
4. T. Bo *et al.*, “Coherent versus Kramers-Kronig transceivers in metro application: A power consumption perspective”, *Proc. of OFC*, M1H.7, 2019.
5. Z. Xing *et al.*, “600G PAM4 transmission using A 4-lambda CWDM TOSA based on controlled-ISI pulse shaping and Tomlinson-Harashima precoding”, *Proc. of ECOC*, Tu.3.D.1, 2019.
6. W. Wang *et al.*, “Demonstration of 214Gbps per lane IM/DD PAM-4 transmission using O-band 35GHz-class EML with advanced MLSE and KP$-FEC”, *Proc. of OFC*, M4F.4, 2020.
7. A. Masuda *et al.*, “96-Gbaud PAM-4 Transmission with 1 sample/symbol under 22-GHz Bandwidth Limitation Using NL-MLSE Based on Third-Order Volterra Filter”, *Proc. of ECOC*, We4G.5, 2018.
8. A. Masuda *et al.*, “255-Gbps PAM-8 transmission under 20-GHz bandwidth limitation using NL-MLSE based on Volterra filter”, *Proc. of OFC*, W4I.6, 2019.

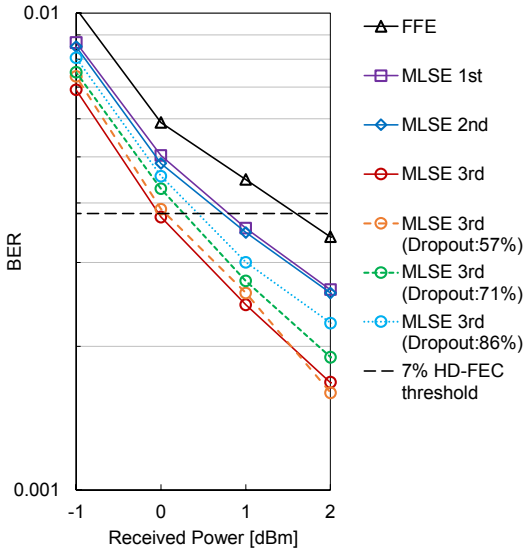

Fig. 5: Transmission performances of 255-Gbps PAM8 signal with 10-km transmission.

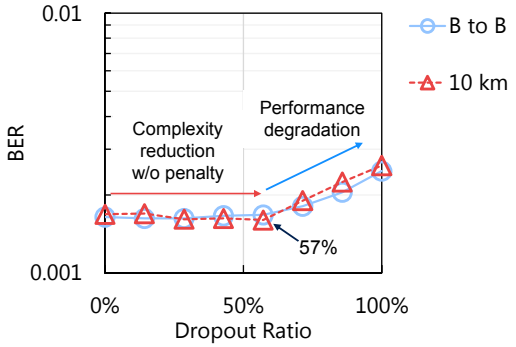

Fig. 6: The relationship between transmission performance and the removal rate of the number of third-order kernels.